The Astrophysical Journal, 754:38 (6pp), 2012 July 20 doi:10.1088/0004-637X/754/1/38

INCIDENCE OF Mg II ABSORPTION SYSTEMS TOWARD FLAT-SPECTRUM RADIO QUASARS

Hum Chand[1] and Gopal-Krishna[2]
[1] Aryabhatta Research Institute of Observational Sciences (ARIES), Manora Peak, Nainital 263 129, India; hum@aries.res.in
[2] NCRA-TIFR, Pune University Campus, Pune 411 007, India; krishna@ncra.tifr.res.in
Received 2012 January 22; accepted 2012 May 14; published 2012 July 3

ABSTRACT

The conventional wisdom that the rate of incidence of Mg II absorption systems, dN/dz (excluding "associated systems" having a velocity βc relative to the active galactic nucleus (AGN) of less than ∼5000 km s^{-1}), is totally independent of the background AGNs has been challenged by a recent finding that dN/dz for strong Mg II absorption systems toward distant blazars is $2.2\pm^{0.8}_{0.6}$ times the value known for normal optically selected quasars (QSOs). This has led to the suggestion that a significant fraction of even the absorption systems with β as high as ∼0.1 may have been ejected by the relativistic jets in the blazars, which are expected to be pointed close to our direction. Here, we investigate this scenario using a large sample of 115 flat-spectrum radio-loud quasars (FSRQs) that also possess powerful jets, but are only weakly polarized. We show, for the first time, that dN/dz toward FSRQs is, on the whole, quite similar to that known for QSOs and that the comparative excess of strong Mg II absorption systems seen toward blazars is mainly confined to $\beta < 0.15$. The excess relative to FSRQs probably results from a likely closer alignment of blazar jets with our direction; hence, any gas clouds accelerated by them are more likely to be on the line of sight to the active quasar nucleus.

Key words: BL Lacertae objects: general – galaxies: jets – intergalactic medium – quasars: absorption lines – quasars: general – techniques: spectroscopic

Online-only material: machine-readable tables

1. INTRODUCTION

The study of Mg II absorption line systems in the spectra of QSOs has provided a means of detecting distant normal field galaxies which happen to be situated close to the lines of sight of the QSOs (e.g., Bergeron & Boissé 1991; Steidel et al. 1994). Barring the so-called associated systems (having $z_{\rm abs} \sim z_{\rm QSO}$), the absorption line systems are customarily believed to arise in intervening structures that are wholly unrelated to the background QSO. This view was, however, challenged by the finding that the occurrence rate, dN/dz, of Mg II absorption systems in the spectra of gamma-ray bursts (GRBs) is nearly four times the value found for QSOs when strong lines having a rest-frame equivalent width >1 Å are considered (Prochter et al. 2006a). Later studies have supported this unexpected trend, but the excess factor was found to be smaller, 2.1 ± 0.6 (Sudilovsky et al. 2007; Vergani et al. 2009; Tejos et al. 2009). More recently, Bergeron et al. (2011, hereafter BBM) examined this issue for the case of blazars that, like GRBs, also possess relativistic jets pointed close to our direction but are considerably less variable. Using intermediate-resolution optical/UV spectra of their sample of 45 powerful blazars (predominantly distant BL Lac objects) at $0.8 < z_{\rm em} < 1.9$, and again excluding "associated systems," these authors found a factor of ∼2 excess (3σ confidence) in the incidence of Mg II absorption systems, as compared to the systems detected toward QSOs. Interestingly, the excess is found both for strong ($w_r \geqslant 1.0$ Å) and weaker (0.3 Å $\leqslant w_r < 1.0$ Å) Mg II systems, where w_r is the rest-frame equivalent width. Thus, the results pertaining to both GRBs and BL Lac objects hint at the radical premise that the observed occurrence of at least the (purportedly intervening) strong Mg II absorption systems is somehow connected with the background source (BBM).

The origin of the above unexpected result is unclear. BBM argued that, while dust extinction can lower the apparent incidence of absorbers toward QSOs and gravitational lensing can increase it toward GRBs and blazars, the expected amplitude of these effects falls short, by at least an order of magnitude, of explaining the aforementioned factor of two discrepancy between the incidence rates of Mg II absorbers found toward blazars/GRBs versus normal QSOs. They further estimated that powerful jets in the blazars are capable of sweeping sufficiently large column densities of gas (up to 10^{18}–10^{20} cm^{-2}) and accelerating such clouds to velocities of order $0.1c$, thereby possibly accounting for the excess of Mg II absorption systems observed in comparison with QSOs. From the observational side, evidence is still lacking for such high-velocity outflows of cool material from radio-loud active galactic nuclei (AGNs), although mildly relativistic outflows of highly ionized gas in the nuclear region now appear to be seen commonly for such sources (e.g., Holt et al. 2008). Based on the observations of Fe XXV/XXVI K-shell resonance lines in the X-ray band, outflow speeds of $\approx 0.15c$ have recently been inferred for highly ionized gas clouds with column densities of $N_{\rm H} \approx 10^{23}$ cm^{-2} located within the central parsec of the AGN (Tombesi et al. 2011). Tombesi et al. argued that clouds with even higher ejection velocities could have remained undetected on account of selection effects and instrumental sensitivity limitations. However, independent evidence of such high-velocity outflows of cool material is still essential in view of the recent finding of Giustini et al. (2011), who detected a highly ionized fast ($v_x \sim 16{,}500$ km s^{-1}) X-ray outflow associated with a slower UV outflow ($v_x \sim 5000$ km s^{-1}).

While the above findings lend some credence to the hypothesis that the observed excess of Mg II absorption systems toward blazars might have a causal relationship to gaseous outflows triggered by their relativistic jets pointed close to our direction (BBM), it would clearly be desirable to probe this suggestion using an independent sample of AGNs having powerful Doppler-boosted jets. Here, we examine this question using such a

Table 1
Basic Data on our Sets of Radio-Loud Quasars (Nonblazar Type FSRQs)

	Data Set	Content	z_{em} Range	Threshold EW (Mg II λ2796)	Instrument(s) Used for Spectroscopy	Limiting Optical Magnitude
1.	Ellison et al. (2004)	75 radio-selected quasars (taken[a] 63)	0.6–1.7	0.3 Å	ISIS (WHT 4m) EFOSC2 (ESO 3.6m) FORS1 (VLT UT3) (Intermediate-resolution)	Unspecified
2.	Bernet et al. (2010)	77 radio-selected quasars (taken[a] 32[b])	0.6–2.0	0.1 Å	UVES (VLT UT2) (High-resolution)	$m_V < 19$
3.	Jorgenson et al. (2006)	68 radio-selected quasars (taken[a] 8)[c]	0.65–1.33	0.02 Å	HIRES (Keck) (High-resolution)	$m_R < 22.0$ (mostly ∼ 18)
4.	Narayanan et al. (2007)	81 QSOs from ESO archive (taken[a] 12)[d]	0.4–2.4	0.02 Å	UVES (VLT UT2) (High-resolution)	$m_g < 21.6$ (mostly < 19)

Notes.
[a] Applying the four selection filters: (1) eliminating the sources that are common to two or more of the samples, (2) excluding all sources that are not in the CRATES catalog of flat-spectrum radio quasars (FSRQs), (3) eliminating sources that are classified as either "HP" or "BL" in Véron-Cetty & Véron (2010) or as "BZB" (implying BL Lac) or "BZU" (implying uncertain type) in the blazar catalog ROMA-BZCAT (2009), and (4) availability of an intermediate- or high-resolution optical spectrum (see Section 2).
[b] Excluding the three quasars (J114608.1−244733, J204719.7−163906, and J213638.6+004154) already covered in data set 1.
[c] The 68 radio-selected quasars in Jorgenson et al. (2006) were used in the survey for damped Lyα systems. Of these, 54 satisfy our selection criteria; for these we made a search for high-resolution spectra in the UVES/VLT and HIRES/Keck archives and found reduced HIRES/Keck spectra for eight of them.
[d] Excluding the five quasars, two of which (J013857.4−225447 and J204719.7−163906) have already been covered in data set 1, with the other three (J095456.8+174331, J113007.0−144927, and J123200.0−022405) covered in data set 2.

sample; however, it consists of a different class of powerful AGNs, namely, flat-spectrum radio quasars (FSRQs, with low optical polarization, hence nonblazar type). Compared with the blazar sample studied by BBM, our sample of 115 (non-blazar) FSRQs is 2.5 times larger, and similar or higher resolution optical/UV spectra are available for all its members from either the literature or various data archives.

2. THE FSRQ SAMPLE AND THE SPECTRAL DATA

Our four data sets of FSRQs were derived from the four publications listed in Table 1. All but the last of these publications (Narayanan et al. 2007) provide samples of radio-selected quasars; the fourth publication is a mix of radio and optical selection (Table 1). To begin, we merged the samples reported in the four publications, obtaining a list of 301 quasars. From this basic list we eliminated the eight quasars present in more than one of the four samples. For instance, if a quasar had already occurred in the first sample, it was deleted from all the remaining samples in which it appeared. From the reduced list of 293 mostly radio-selected quasars, we then excluded all those not contained in the CRATES catalog of FSRQs, which provides for each source the spectral index,[3] α, between 1.4 GHz and 4.8 GHz and contains only sources with $\alpha > -0.5$ and a flux density above 65 mJy at 4.8 GHz (Healey et al. 2007). This selection filter left us with 201 FSRQs. From this list we further deleted sources that are classified as either "HP" or "BL" in the Véron-Cetty & Véron (2010) catalog, or as "BZB" (implying BL Lac) or "BZU" (implying uncertain type) in the catalog ROMA-BZCAT 2009 (Massaro et al. 2009). Lastly, we excluded all sources which are absent from both of these catalogs, treating their nature as uncertain. This sequence of selection filters left us with 163 FSRQs (nonblazars), i.e., 65, 32, 54, and 12 FSRQs constituting our data sets 1, 2, 3, and 4, respectively, drawn from the four parent publications mentioned in Table 1.

For the largest data set 1 (65 southern FSRQs), the parent publication (Ellison et al. 2004) has already provided for all but two sources (J043850.5−201226/B0436−203 and J165945.0+021307/B1654−020) all of the information relevant for the present study, such as Mg II absorber redshift, rest-frame equivalent width EW(Mg II λ2796), and the redshift path values for systems having EW(Mg II λ2796) above the thresholds 0.3 Å, 0.6 Å, and 1.0 Å (their Table 3). Following an unsuccessful search for the optical spectra of the two remaining sources in the UVES/Very Large Telescope (VLT) archive, both sources were excluded from further analysis. For the sources in the remaining three data sets (nos. 2–4), a similar archival search for high-resolution optical spectra was much more crucial, since the requisite information was not available in their parent publications (Table 1).

For the southern data set 2, spectra of all 32 FSRQs were found in the UVES/VLT[4] archive. For the northern data set 3, a search was made in the HIRES/Keck[5] archive and spectra for 10 out of the total 54 FSRQs were found. However, for one of them (J064204+675836), only raw science frames were available and the calibration file was missing. For another FSRQ (J185230+401907), only two exposures of the HIRES/Keck observation were available, resulting in a low signal-to-noise ratio (S/N < 10) and hence a much reduced spectral coverage. We thus ended up with eight FSRQs with useful spectra, out of the total of 54 FSRQs in data set 3. Lastly, spectra for all 12 FSRQs in our data set 4 were found in the UVES/VLT archive. This selection process left us with 115 FSRQs (nonblazar type) with high-quality optical/UV spectra, contributed by 63, 32, 8, and 12 FSRQs out of data sets 1, 2, 3, and 4, respectively (Table 1). For post-processing of the extracted spectra of the FSRQs belonging to data sets 2–4, such as air to vacuum wavelength conversion, heliocentric correction, combining individual exposures to enhance the signal-to-noise

[3] α is defined as: flux $\propto$ (frequency)$^{\alpha}$.

[4] http://archive.eso.org/eso/eso_archive_adp.html
[5] https://koa.ipac.caltech.edu/cgi-bin/KOA/nph-KOAlogin

Table 2
Basic Properties of our Sample of 115 (Nonblazar) FSRQs

Quasar Name	z_{em}[a]	α_{radio}	f(4.8 GHz) (mJy)	mag[b]	Filter[b]	Weak Systems Δz	Weak Systems N_{sys}	Strong Systems Δz	Strong Systems N_{sys}	Ref. Code (See Table 1)
J001130.5+005551	2.308620	−0.142	140	19.10	*V*	1.1656	0	1.1656	0	4
J001602.4−001225	2.086940	−0.443	645	18.36	*V*	1.0823	0	1.0823	0	4
J001708.5+813508	3.366000	−0.200	551	16.52	*V*	0.5544	0	0.5544	0	3
J004057.6−014632	1.178000	−0.017	581	18.30	*O*	0.9942	1	0.9942	0	2
J004201.2−403039	2.478000	0.336	299	19.93	*P*	0.0114	0	0.7135	1	1
...	...	...	...	...	...	...	...	...	...	...

Notes.
[a] Based on NASA/IPAC Extragalactic Database (NED).
[b] Based on Véron-Cetty & Véron (2010).

(This table is available in its entirety in a machine-readable form in the online journal. A portion is shown here for guidance regarding its form and content.)

Table 3
Mg II Absorption Systems and Their Rest-Frame Equivalent Widths, w_r(Mg II λ2796 Å), for our Sample of 115 (Nonblazar) FSRQs

FSRQ	z_{em}	z_{abs}	w_r(2796 Å) (Å)	α_{radio}	f(4.8 GHz) (mJy)	∼S/N Per FWHM	Ref. Code (See Table 1)
J004057.6−014632	1.1780	0.6828	0.36 ± 0.01	−0.02	581.0	22.2	2
J004201.2−403039	2.4780	0.8483	2.35 ± 0.15	+0.34	299.0	...	1
J005108.2−065002	1.9750	1.4919	0.90 ± 0.03	−0.08	841.0	...	1
J005108.2−065002	1.9750	1.5698	0.32 ± 0.03	−0.08	841.0	...	1
J024008.2−230916	2.2230	1.3652	1.86 ± 0.01	−0.46	3630.0	261.1	4
...	...	...	... ± ...	...	...	...	...

(This table is available in its entirety in a machine-readable form in the online journal. A portion is shown here for guidance regarding its form and content.)

ratio (S/N), and continuum fitting, we followed the procedure described in Chand et al. (2004). Details of our final sample of 115 FSRQs are given in Table 2.

3. ANALYSIS

Although both UVES and HIRES spectrographs provide a large wavelength coverage, from ∼3000 Å to ∼10000 Å, the available spectral coverage varies from quasar to quasar, based on the choice of cross-disperser settings. Combining exposures from various settings, therefore, sometimes resulted in gaps in the wavelength coverage. In addition, we systematically excluded the following spectral path lengths from our formal search for Mg II absorption systems: (1) the wavelength region blueward of the Lyα emission line to avoid contamination by the Lyα forest, (2) wavelength regions within 5000 km s^{-1} of the Mg II λλ2796, 2803 emission lines at the quasar redshift, as any absorption lines within this velocity interval have a higher probability of being associated with the quasar itself (Section 1), and (3) spectral regions polluted by the various known atmospheric absorption features, which were eliminated by eye for any line blending. Further, noisy spectral regions got discarded by our considering only the spectral ranges with S/N sufficient to detect with >5σ significance any absorption line above the adopted EW threshold (which is 0.3 Å for weak systems and 1.0 Å for strong systems); this is also the criterion used in Ellison et al. 2004 (the parent paper for our data set 1).

In searching for Mg II absorption systems within the included redshift path in each quasar spectrum, we first plotted the normalized spectrum and then plotted over it the same spectrum by shifting the wavelength array by a factor of λ2796.3543/λ2803.5315. Small spectral segments of about 50 Å were then visually inspected for comparable profile shapes and for a doublet ratio between 1:1 and 2:1. To further ascertain the detection of the absorption system, we then searched for corresponding metal lines (e.g., Fe II, Mg II, C IV, Si IV, etc.) in the velocity plot. Weak Mg II doublets that were found within 500 km s^{-1} of each other were taken to be part of the same absorption system and were therefore classified as one multi-cloud system, as is usually done.

From the above analysis of the optical spectra of the total 52 FSRQs drawn from data sets 2–4, we detected 29 Mg II absorption systems with 0.3 Å $\leqslant w_r(2796) <$ 1.0 Å (weak systems) and 10 Mg II absorption systems with $w_r(2796) \geqslant$ 1.0 Å (strong systems). Thus, including data set 1, the total counts of weak and strong Mg II absorption systems in our final sample of 115 FSRQs became 53 and 22, respectively (Table 3). The detected Mg II absorbing system(s) have z_{abs} range, median redshift, and redshift dispersion, respectively, of $0.399 < z_{abs} < 2.638$, 1.119, and 0.499 for the weak systems and $0.238 < z_{abs} < 1.969$, 0.828, and 0.442 for the strong absorption systems.

Table 4 summarizes the results for our final sample of 115 FSRQs, giving $dN/dz = N_{obs}/\Delta z$, where N_{obs} is the number of the observed Mg II absorption systems within the redshift path Δz, for both strong and weak Mg II systems. The errors in dN/dz are calculated based on Poisson statistics for small numbers, with the limits corresponding to the 1σ confidence level of a Gaussian distribution, as tabulated by Gehrels (1986).

4. SUMMARY AND DISCUSSION

It is interesting to note from Table 4 that dN/dz for FSRQs and normal QSOs is quite similar for both weak and strong

Table 4
Comparison of Mg II Absorption Systems Toward FSRQs and Blazars

Absorber Type	$w_r(2796)$ Range	N_{obs}	Δz^a	$\langle z \rangle$	$\frac{dN}{dz}$	$(\frac{dN/dz}{(dN/dz)_{qso}})$	$\eta(\langle z \rangle)^b$	$(\frac{\eta(\langle z \rangle)(dN/dz)}{(dN/dz)_{Blz}})^c$
Weak systems	$0.3\,\text{Å} \leqslant w_r(2796) < 1.0$	53	80.23	1.12 ± 0.42	$0.66^{0.10}_{0.09}$	$1.40^{0.22}_{0.19}$	0.91	$0.79^{0.27}_{0.19}$
Strong systems	$1.0\,\text{Å} \leqslant w_r(2796)$	22	106.02	1.09 ± 0.42	$0.21^{0.05}_{0.04}$	$0.85^{0.22}_{0.18}$	0.81	$0.39^{0.19}_{0.12}$

Notes.
[a] Redshift path estimated for the specified EW detection threshold above the 5σ significance level.
[b] The scale factor $\eta(\langle z \rangle)$ is used for scaling our computed dN/dz for the FSRQ weak and strong absorption systems, from their respective mean redshifts (Column 5) to the mean redshift of the BBM blazars ($\langle z \rangle = 0.83$ for the weak and 0.82 for the strong Mg II absorption systems). For details, see the text in the beginning of Section 4.
[c] $(dN/dz)_{Blz} = 0.76^{0.22}_{0.17}$ at $\langle z \rangle = 0.83$ for the weak absorption systems and $(dN/dz)_{Blz} = 0.43^{0.16}_{0.12}$ at $\langle z \rangle = 0.82$ for the strong absorption systems detected toward the BBM blazars (their Equations (5) and (8)).

Mg II absorption systems (e.g., see Column 7 of Table 4). Here, to compute dN/dz for normal QSOs at the mean redshift of our FSRQs sample, we use the fit of z versus dN/dz for the strong absorption system ($w_r(2796) \geqslant 1.0$ Å), as given by Prochter et al. (2006b; see also Equation (6) of BBM), and for $w_r(2796) \geqslant 0.3$ Å systems as given by Nestor (e.g., see Equation (2) of BBM; Bergeron et al. 2011, private communication), derived in both cases using the QSOs in the Sloan Digital Sky Survey (Data Release 4). Thus, for weak systems toward QSOs, dN/dz at any redshift can be computed by taking the difference between the above two fits (i.e., dN/dz for $w_r(2796) \geqslant 0.3$ Å minus dN/dz for $w_r(2796) \geqslant 1.0$ Å). However, to carry out the comparison with the result reported by BBM for blazars (e.g., see Column 9 of Table 4), which has a different mean redshift compared the mean redshift of our FSRQs sample (e.g., see Column 5 of Table 4), we have to first take into account the known cosmological evolution of dN/dz by scaling our dN/dz values found for the FSRQs to the mean redshift of the Mg II absorption systems toward the BBM blazars ($\langle z \rangle = 0.83$). To do this scaling, we assumed that the cosmological evolution of dN/dz for our FSRQ sample is similar to that known for dN/dz toward QSOs, which seems reasonable considering (1) the lack of dN/dz evolution studies for radio-loud quasars and (2) that our dN/dz estimated for FSRQs appears quite similar to that known for QSOs (see above). The computed scale factors, $\eta(\langle z \rangle)$, are listed in Column 8 of Table 4. By multiplying by these scale factors, our computed values of dN/dz for the FSRQ subsets are scaled to the (slightly lower) mean redshift of the BBM blazar sample ($\langle z \rangle = 0.83$) before the ratio of dN/dz for our FSRQ subsets and the corresponding BBM blazar sets are taken (Column 9 of Table 4).

The most interesting result from Table 4 is that for Mg II strong absorption systems, dN/dz for FSRQs is only about half of the value reported by BBM for blazars, which they showed to be itself nearly twice the value known for optically selected quasars (QSOs, which are mostly radio quiet). In other words, the excess abundance of Mg II strong absorption systems seen toward blazars (and also GRBs), in comparison with QSOs (BBM and references therein), does not seem a characteristic of FSRQs of the nonblazar type, even though they too possess powerful Doppler-boosted jets. BBM suggested that the excess seen toward blazars might be due to absorbing gas clouds swept up by the powerful jets and accelerated to mildly relativistic velocities (Section 1). While this might readily explain the excess of the absorption systems relative to normal quasars (i.e., optically selected, mostly radio-quiet, QSOs) that lack powerful jets, can this be reconciled with the lack of excess found here for FSRQs that do possess powerful relativistic jets? A relevant factor here is the likelihood that, compared with blazars (and GRBs), the jets in FSRQs may be less well aligned to the line of sight. A plausible outcome of such a jet orientation scenario, which underlies a popular class of unification models of radio-loud AGNs (e.g., Orr & Browne 1982; Antonucci & Ulvestad 1985; Wills & Browne 1986), would be that any gas clouds accelerated by the powerful FSRQ jets to extremely high (even mildly relativistic) speeds may simply not appear in the foreground of the quasar nucleus and hence escape detection as absorption systems.

To probe this hypothesis, we now compare for the FSRQs and blazars the distributions of speeds, β, of the observed Mg II absorption-line systems, relative to the parent quasar/blazar, where

$$\beta \equiv \frac{v}{c} = \frac{(1+z_{em})^2 - (1+z_{abs})^2}{(1+z_{em})^2 + (1+z_{abs})^2}. \quad (1)$$

To make a meaningful comparison, we have derived a subset from our FSRQ sample by taking only those 15 FSRQs that satisfy the constraints that (1) the emission redshift, z_{em}, falls within the range $0.875 < z_{em} < 1.715$ of the 33 BBM blazars actually showing Mg II absorption systems (out of the total 45 blazars listed in Table 2 of BBM)) and that (2) the detected Mg II absorption systems satisfy $0.350 < z_{abs} < 1.430$ (for weak systems) and $0.350 < z_{abs} < 1.579$ (for strong systems) as the z_{abs} ranges for the 33 BBM blazars. To begin, histograms of z_{em} for the subset of these 15 FSRQs and the 33 BBM blazars are compared in Figure 1. The Kolmogorov-Smirnov (K-S) test shows with 84.8% probability that the two histograms are drawn from the same intrinsic distribution of z_{em}. In view of the known cosmological evolution of dN/dz, this prior confirmation of redshift matching is important. After the above matching of the redshift range both in z_{em} and z_{abs}, which led to our subset of 15 FSRQs for comparison with the 33 BBM blazars, we are left with 14 weak and 3 strong Mg II absorption systems seen toward our 15 FSRQs, to be compared with the 19 weak and 13 strong Mg II absorption systems detected toward the 33 BBM blazars. The two panels in Figure 2 compare β distributions for the redshift-matched subsets of our FSRQs and BBM blazars separately for the weak and strong Mg II absorption systems (recall that "associated systems" having $\beta < 0.017$ have already been excluded; Section 3). The unpaired t-test probabilities that the β distributions for blazars and FSRQs are drawn from the same parent population are 99.99% and 1.3% for the weak and strong absorption systems, respectively. Here, the unpaired t-test is preferred over the K-S test, in view of the small sample size of the absorption systems, especially the strong systems. Thus,

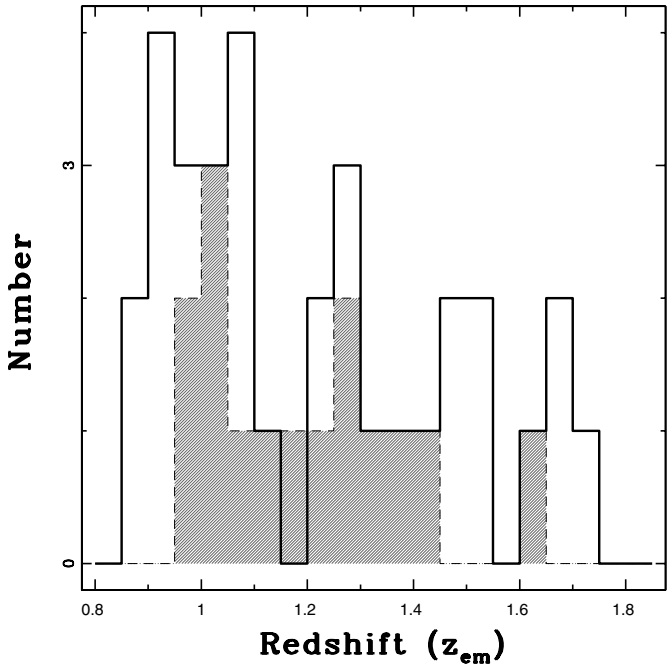

Figure 1. Histograms in emission redshift; the solid line is for the 33 BBM blazars with detected Mg II absorbing systems (their Table 2). The shaded region is for our subset of 15 FSRQs fulfilling the constraints that (1) emission redshift, z_{em}, falls within the range $0.875 < z_{em} < 1.715$ of the 33 BBM blazars and that (2) the detected Mg II absorbing system(s) have z_{abs} in the range applicable to the BBM blazars, namely, $0.350 < z_{abs} < 1.430$ for weak systems and $0.350 < z_{abs} < 1.579$ for strong absorption systems. The K-S test shows with 84.8% probability that the two histograms are drawn from the same parent distribution of z_{em}.

the difference between the strong absorption systems toward blazars and FSRQs appears statistically significant, although larger data sets would clearly be very desirable. As seen from Figure 2 (right panel), the main contributor to the difference between the two β-distributions is the conspicuous presence of strong absorption systems for the BBM blazars at β values up to 0.15. Interestingly, BBM reported a similar excess of strong Mg II absorption systems toward their blazars in comparison with QSOs (their Figure 4), which they interpret by postulating high-speed outflowing clouds of cool gas accelerated by the powerful blazar jets (Section 1). While the FSRQs studied here also possess powerful jets, the deficit of strong absorption systems at lower β is still present, in comparison with blazars (Figure 2, right panel). As noted above, a plausible way to reconcile this with the BBM hypothesis is then to consider the possibility that the FSRQ jets are less closely aligned to our direction, compared with the jets in the BBM blazars that are also powerful and are expected (by definition) to be strongly polarized. Such an inference was indeed drawn by Valtaoja et al. (1992), based purely on their extensive radio flux monitoring data at centimeter wavelengths, which showed that, on average, low-polarization quasars (FSRQs) vary with a smaller amplitude and on a longer timescale compared with blazars (see, also, Orr & Browne 1982). One would then expect that any ultra-fast-moving absorbing clouds accelerated by powerful FSRQ jets would mostly be out of the line of sight of the quasar nucleus. This suggestion can be tested by the analysis of Mg II absorption systems toward steep-spectrum quasars whose jets are expected to be even less well aligned to our direction (e.g., Barthel 1999; Orr & Browne 1982).

Another hint favoring such an orientation-based explanation comes from the radio properties of the small minority of FSRQs that have been detected with the Large Area Telescope (LAT) on board the *Fermi Gamma-ray Space Telescope* (see Linford et al. 2011). These authors find that the γ-ray bright LAT FSRQs are extreme sources with higher core brightness temperature and greater core polarization, as well as a larger (apparent) opening angle of the parsec-scale jets, than their non-LAT counterparts. Interpreting these differences, they suggested that the γ-ray loud FSRQs can be explained by Doppler boosting, but the jet orientation and/or speeds must be significantly different for the γ-ray quiet FSRQs (which show weaker polarization). This scenario would be consistent with the above assumption that the jets in our sample of (weakly polarized, hence nonblazar) FSRQs may be less closely aligned to the line of sight, in comparison with the similarly powerful jets in the BBM blazars. Although such a bias may well explain the difference between

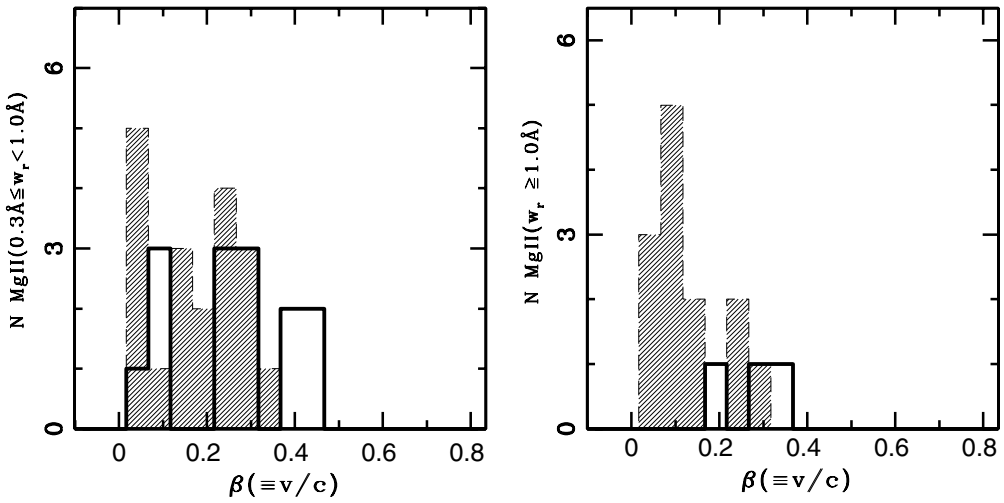

Figure 2. Left: histogram of the weak ($0.3\,\text{Å} \leqslant w_r(2796) < 1.0\,\text{Å}$) "intervening" Mg II absorption systems toward the FSRQs, w.r.t. the velocity of the absorber relative to the background FSRQ (Equation (1); thick black curve). The shaded region shows the corresponding histogram of the weak Mg II absorption systems found toward the BBM blazars, adopting the incidence of these systems as given in Bergeron et al. (2011). Right: same as the left panel, but for strong Mg II absorption systems ($w_r(2796) \geqslant 1.0\,\text{Å}$). This comparison is carried out using a subset of 15 FSRQs drawn from our FSRQ sample by applying a redshift matching procedure described in Section 4 after excluding the systems with $\Delta v < 5000$ km s^{-1}, i.e., $\beta < 0.017$.

the occurrence rates of strong Mg II absorption toward powerful blazars and FSRQs/QSOs, further substantiation of this trend employing larger data sets would greatly strengthen the BBM scenario that strong Mg II absorption systems may often reveal the most extreme velocity outflows of cool gas clouds from powerful AGNs, underscoring the need to investigate the wide-ranging theoretical implications of this phenomenon.

This research made use of (1) the Keck Observatory Archive (KOA), which is operated by the W. M. Keck Observatory and the NASA Exoplanet Science Institute (NExScI), under contract with the National Aeronautics and Space Administration, using observations made using the HIRES spectrograph at the Keck, Mauna Kea, HI; (2) ESO Science Archive Facility by using observations made using the UVES spectrograph at the VLT, Paranal, Chile, and (3) the NASA/IPAC Extragalactic Database (NED), which is operated by the Jet Propulsion Laboratory, California Institute of Technology, under contract with the National Aeronautics and Space Administration.

We thank the anonymous referee for the constructive criticism and helpful suggestions. We gratefully acknowledge the help from T. Parasakthi with the processed data for the quasars belonging to our data set 4, and that from Ravi Joshi in resolving some issues related to the archival data used here.

Facilities: Keck:I (HIRES), VLT:Kueyen (UVES)

REFERENCES

Antonucci, R. R. J., & Ulvestad, J. S. 1985, ApJ, 294, 158
Barthel, P. D. 1999, in ASP Conf. Ser. 162, Quasars and Cosmology, ed. G. Ferland & J. Baldwin (San Francisco, CA: ASP), 127
Bergeron, J., & Boissé, P. 1991, A&A, 243, 344
Bergeron, J., Boissé, P., & Ménard, B. 2011, A&A, 525, A51
Bernet, M. L., Miniati, F., & Lilly, S. J. 2010, ApJ, 711, 380
Chand, H., Srianand, R., Petitjean, P., & Aracil, B. 2004, A&A, 417, 853
Ellison, S. L., Churchill, C. W., Rix, S. A., & Pettini, M. 2004, ApJ, 615, 118
Gehrels, N. 1986, ApJ, 303, 336
Giustini, M., Cappi, M., Chartas, G., et al. 2011, A&A, 536, A49
Healey, S. E., Romani, R. W., Taylor, G. B., et al. 2007, ApJS, 171, 61
Holt, J., Tadhunter, C. N., & Morganti, R. 2008, MNRAS, 387, 639
Jorgenson, R. A., Wolfe, A. M., Prochaska, J. X., et al. 2006, ApJ, 646, 730
Linford, J. D., Taylor, G. B., Romani, R. W., et al. 2011, ApJ, 726, 16
Massaro, E., Giommi, P., Leto, C., et al. 2009, A&A, 495, 691
Narayanan, A., Misawa, T., Charlton, J. C., & Kim, T.-S. 2007, ApJ, 660, 1093
Orr, M. J. L., & Browne, I. W. A. 1982, MNRAS, 200, 1067
Prochter, G. E., Prochaska, J. X., & Burles, S. M. 2006a, ApJ, 639, 766
Prochter, G. E., Prochaska, J. X., Chen, H.-W., et al. 2006b, ApJ, 648, L93
Steidel, C. C., Dickinson, M., & Persson, S. E. 1994, ApJ, 437, L75
Sudilovsky, V., Savaglio, S., Vreeswijk, P., et al. 2007, ApJ, 669, 741
Tejos, N., Lopez, S., Prochaska, J. X., et al. 2009, ApJ, 706, 1309
Tombesi, F., Cappi, M., Reeves, J. N., et al. 2011, ApJ, 742, 44
Valtaoja, E., Terasranta, H., Urpo, S., et al. 1992, A&A, 254, 80
Vergani, S. D., Petitjean, P., Ledoux, C., et al. 2009, A&A, 503, 771
Véron-Cetty, M.-P., & Véron, P. 2010, A&A, 518, A10
Wills, B. J., & Browne, I. W. A. 1986, ApJ, 302, 56